Pergamon

Cement and Concrete Research, Vol. 26, No. 6, pp. 869-881, 1996

0008-8846/96 $15.00 + .00

PII S0008-8846(96)00072-5

EFFECT OF CRACKING AND HEALING ON CHLORIDE TRANSPORT IN OPC CONCRETE

Stefan Jacobsen[1], Jacques Marchand[2] and Luc Boisvert[2]
1) Norwegian Building Research Institute, Oslo, Norway
2) Université Laval/CRIB, Québec, Canada

(Refereed)
(Received October 19, 1995; in final form April 9, 1996)

ABSTRACT

The effects of cracking and self healing on chloride migration and compressive strength were investigated on w/c = 0.40 concrete. Internal cracking due to rapid freeze/thaw exposure resulted in a compressive strength reduction of 68 - 40 % and a reduced Ultrasonic Pulse Velocity (UPV) to 78 - 45 % of undamaged values. The rate of chloride migration through 15 mm thick slices under a 10 volt electric field was increased by 2.5 - 8 times, and the chloride penetration time through the slices was reduced from 64 to 0 hours for the most severe cracking. The increased chloride transport due to cracking could be predicted fairly well by characterizing the cracks using a square grid crack pattern model. Self healing by storage of cracked specimens in lime saturated water at 20 °C for three months after stop of freeze/thaw exposure gave recovery in UPV of 50 - 100 %, but compressive strength recovered only 0 - 10 % of the initial value. Rate of chloride migration in the self-healed concretes was reduced by 28 - 35 %, and penetration time was increased compared to newly cracked concrete. The chloride migration through an air entrained concrete with the same w/c ratio (no internal cracking after more than 300 cycles of rapid freeze/thaw exposure), was unaffected by freeze/thaw.

Introduction and Background

Cracks in concrete structures can have negative effects on important parameters such as permeability, rate of chloride ingress and thus reinforcement corrosion protection. It is normally assumed that smaller cracks are of less importance to durability than larger cracks. Construction codes often specify maximum tolerable crack widths in the range 0.2 - 0.3 mm.

In some previous investigations (1,2), freeze/thaw induced cracks and their self healing were studied, and some previous research on self-healing of cracked concrete was reviewed. It was found that pulse velocity and resonance frequency values could recover up to 100 % of values of undamaged concrete after storing cracked concrete in water for three months. The compressive

strength, however, showed smaller recovery after self healing. It was shown that the recovery was associated with a self-healing process where microcracks were locally filled up by newly formed hydration products. These products, mainly of CSH-type, were able to bridge several cracks with widths smaller than approximately 5 μm. Investigations of pore structure by mercury intrusion porosimetry and low temperature calorimetry (3,4) showed that the self-healing reduced the increase in porosity due to cracking, both in very small pores ("gel size range") and in larger pores/cracks.

The effect of cracks and crack healing on mass transport processes have been the subject of a few studies in recent years. Studies of reduced permeability/water flow in concrete cracks due to self-healing were performed by Clear (5), Ripphausen (6) and Meischner (7). They found that water flow in cracks up to ca 0.3 mm crack width could come to a complete stop after some time. This crack width is much larger than what was observed due to frost deterioration in (2): 1 - 10 μm. Hearn (8) observed that the increased permeability in dried/resaturated concrete could also be reduced over time. Arnold and Johnson (9) observed reduced flow through cracks in concrete dams over time. They attributed this to sealing of the cracks.

Increased chloride transfer in concrete due to load induced cracking was observed by Samaha and Hover and by Locoge et al (10, 11). Fidjestøl and Nilsen (12), Bakker (13) and Sandberg and Tang (14) discussed possible reduction of chloride ingress and corrosion rate in cracked concrete due to crack-healing. However, none of them compared systematically chloride transport in concrete with "fresh" and "healed" cracks. Dry (15) developed and investigated various systems for self-repair of cracks: so-called smart materials with hollow fibres containing repairing chemicals. When released at cracking of the concrete, these chemicals were able to give the repaired crack better mechanical properties and permeability than the sound material.

Research Significance

The present study has been undertaken since little information exists on the effect of cracking and self healing on chloride transfer. Well cured OPC concrete has been cracked to various degrees by rapid freeze/thaw exposure. Ultrasonic pulse velocity, compressive strength and chloride migration measurements were then performed on undamaged, cracked and self healed specimens. The self-healing took place in lime saturated water after stop of freeze/thaw.

Materials, Concrete Mixing and Specimens

Two concrete mixtures with w/c = 0.40 with (A) and without air entraining agent (NA) were made with slump values of 70 and 90 mm. A Canadian Ordinary Portland Cement type 10 was used. The aggregate consisted of natural sand (0 - 5 mm) and coarse aggregate (0 - 10 mm) of granite origin, the admixtures were a naphtalene based superplasticizer, and a fatty acid air entraining agent.

The concretes were batched in a horizontal rotating counter current pan mixer. The mixing procedure consisted of 1 minute mixing of dry materials, 3 minutes with water and 2 minutes stop, and finally 2 minutes remixing before determining properties of fresh concrete and moulding specimens. Admixtures were mixed in separate portions of the water, and separately added in the mixture. Cylinders of 101.6 × 203.2 mm (= 4 × 8 inches diameter × height) were made for compressive strength measurements, and some cylinders with diameter 95 mm were

TABLE 1
Concrete Mixes (kg/m^3)

Material/property	NA	A
Cement (type 10)	433	408
Water	173	163
W/C	0.40	0.40
sand (0 - 5 mm)	792	747
coarse (0 - 10 mm)	1070	1009
SP (SPN)	242 ml	200 ml
AEA (Microair)	-	12 ml
Fresh concrete:		
Slump	90 mm	70 mm
Air	3.0 %	6.2 %
Density	2468	2327
Air void characteristics ASTM C457		
Air (%)	1.3 %	3.9 %
α (Specific surface)	12.4 mm^{-1}	26.1 mm^{-1}
$\bar{L}$ (Air void spacing factor)	0.70 mm	0.19 mm
Paste	25.6 vol-%	22.9 vol-%

made for chloride migration measurements. The cylinders were stripped after 24 hours and cured in a fog room (100 % relative humidity) for four months prior to the freeze/thaw testing.

Concretes

Table 1 gives concrete composition, fresh concrete properties and air void characteristics according to ASTM C457 - modified point count. Table 2 gives cement characteristics. Table 3 gives compressive strength (three parallel cylinders).

Experimental Procedures

Freeze/Thaw Testing and Self Healing. Rapid freeze/thaw testing can introduce cracks in a controlled fashion, as indicated by measuring the pulse velocity increase as function of freeze/thaw cycles for a particular concrete and exposure condition. In the present experiments freeze/thaw cycling was performed according to a modified ASTM C666 procedure B (freezing in air, thawing in water) (16). The modification consists of wrapping the specimens in cloths to keep them moist during the freezing part of the freeze/thaw cycle. Double fibre reinforced heavy paper cloths were kept around the specimens with rubber bands. The freeze/thaw chamber produced 8 cycles pr. day within the limits of ASTM C666.

TABLE 2
Cement Characteristics (% by Mass)

SiO_2	Al_2O_3	TiO_2	P_2O_5	Fe_2O_3	CaO	Na_2O	K_2O	SO_3	L.O.I.	Blaine (m^2/kg)
20.72	4.24	0.22	0.21	2.96	62.43	0.31	0.81	3.12	2.25	401

The surfaces of the cylinders for compressive strength measurements were ground before freeze/thaw cycling. At three months age two single NA cylinders (Pilot 1 and Pilot 2, see figure 2) were tested, in order to know the exact evolution of UPV during freeze/thaw. then, at four months age, all specimens were subjected to freeze/thaw cycles. During freeze/thaw cycles the weight (in air and water), UPV and compressive strength of the cylinders were measured regularly. Three freeze/thaw specimens and one reference kept continuously in the fog room were monitored for each mix.

Specimens for compressive strength and chloride migration measurements were taken after 0, 31, 61 and 95 cycles for the NA-concrete, and 0, 95 and 316 cycles for the A-concrete. For each variable, three parallel cylinders for compressive strength were used, and two slices were tested for chloride migration.

Investigations of effect of self-healing on compressive strength and chloride migration were performed on NA-specimens exposed to 31, 61 and 95 cycles, and subsequently stored in lime saturated water for three months. Slices for chloride migration tests were sawn from the cracked cylinders before self healing in water. This increased the surface/volume ratio 3.4 times, and reduced minimum half size from 4.75 cm (radius of cylinder) to 0.75 cm (half thickness of slice).

Measurements of Crack Density. The crack density caused by rapid freeze/thaw exposure was measured on polished sections impregnated with a red dye, Hornain et al. (17). The impregnation procedure involves no drying that may increase the microcracking. Two polished sections were made at each level of deterioration: 0, 31, 61 and 95 freeze/thaw cycles. Crack densities were measured by counting number of cracks traversing parallel lines of approximately 5 mm distance. 1500 mm traverse length was counted for each level of deterioration.

Chloride Migration Testing. Several test methods exist for testing of the chloride migration in concrete (sometimes called chloride permeability). These are accelerated tests where the driving force is an electrical potential that forces all ions (not only chlorides) to migrate between the anode and the cathode. The most well known is Whitings test (18). It consists in measuring the total current passing through a concrete sample placed in a cell with an upstream solution of 0.5 M NaCl and a downstream solution of 3 M NaOH. A 60 volt potential is applied over the specimen. Following (18) other methods have been proposed e.g. (19) and (20). In (21-24) reviews and equations relevant for testing of migration are given. The total flux J, (mol/(cm^2·s)) during migration is given by the Nernst-Planck equation (1):

$$J = -D\frac{\partial C(x)}{\partial x} + M\frac{zFEC(x)}{RT} \qquad (1)$$

TABLE 3
Compressive Strength at Freeze/Thaw and Healing in Water (3 Months)

	28 day	Freeze/thaw exposure					3 months in water		
		0 cy 1)	31 cy	61 cy	95 cy	316 cy	31 cy	61 cy	95 cy
NA (MPa)	49.2	**56.9** 2)	**38.7**	**30.8**	**22.7**	-	**44.2**	**31.2**	**21.7**
(% of $f_{c\,0\,cy}$)	87	100	**68**	**54**	**40**		**78**	**55**	**38**
A (MPa)	36	44.3	-	-	44.1	43.9	-	-	-
(% of $f_{c\,0\,cy}$)	81	100			100	99			

1) 4 months 2) 2 parallel specimens only

The first part of the right side of (1) (Ficks first law) takes into account pure diffusion, with D diffusion coefficient (cm^2/s) and $\partial C/\partial x$ concentration gradient ($mol/(cm^3 \cdot cm)$). The second part of the right side of (1) quantifies the contribution from migration due to the electric field.

where

M: Migration coefficient (cm^2/s)
J: Unidirectional flux of chloride ions ($mol/(cm^2 \cdot s)$)
R: The gas constant (8.314 J/(mol·K))
T: Absolute temperature (293 K)
F: Faradays number (96500 J/V)
z: Valency of ion (1 for Cl^-)
C(x): Chloride concentration (mol/cm^3)
E: Potential applied over the specimen (V/m)

Assuming the contribution from diffusion to be negligible compared to migration at 10 V is reasonable according to Streicher and Alexander (21). Then, only taking into account the migration due to the electrical field, the migration coefficient M can be calculated by rearranging the last term of equation (1):

$$M = \frac{JRTl}{zFCE} \tag{2}$$

A constant mass transfer coefficient is not necessarily the case due to chloride binding in the cement hydrates, Nilsson et al (25). However, during steady state flow a constant M is assumed. Steady state was obtained 0 - 3 days after start, depending on concrete/degree of cracking.

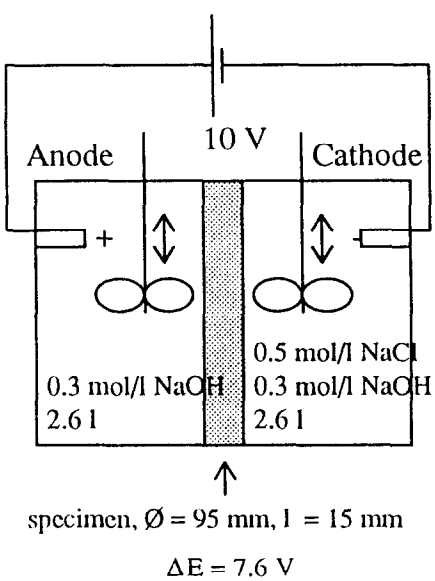

FIG. 1.
Chloride migration test-set-up.

Fifteen mm thick slices for chloride migration testing were wet sawn with a diamond blade from the 95 mm diameter cylinders after various degrees of cracking (l = 1.5 cm in equation (2)). Before inserting the specimens in the migration cells, the slices were kept in water under vacuum for two days. The pump was kept running at day and stopped at night, and produced a vacuum of 0.01 atmosphere. To check the effect of the vacuum on absorption and chloride migration, some test series were duplicated with chloride migration through slices submerged in water under atmospheric pressure only, for two days before testing. All slices were weighed before and after vacuum treatment or submersion.

A chloride migration method recently developed at Laval University was used (27). Figure 1 shows the test principle. Two parallel specimens were used for each variable investigated. Silicone was used to ensure tightness between the concrete and the migration cell. The applied voltage was 10 V between the electrodes. The potential measured between the concrete surfaces of the upstream and downstream sides was 7.6 V (= E in equation (2)). The electrochemical explanation for this drop has been discussed by Gerard and Marchand, (26). 2.6 litres of solution (distilled, deareated water) were used in each of the compartments: 0.5 mol $NaCl^-/l$ (approximately 3 % NaCl, C = $5 \cdot 10^{-4}$ mol/cm^3 in equation (2)), and 0.3 mol NaOH/l (1.2 % NaOH) on the upstream side, and 0.3 mol NaOH/l on the downstream side. The solutions were stirred slowly during test to release air bubbles from the surface of the concrete. The anode was made of a titanium-ruthenium oxide composite, which was chosen due to high conductivity and stability in severe electrochemical environment, (27). The cathode was made of graphite. The chloride concentration in the downstream cell was measured using potentiometric titration at various intervals for about 3 weeks after a steady-state flow was obtained. Measurements were also made in the upstream cell for correction, when the chloride concentration fell below 0.45 mol Cl^-/l. This was done since some researchers have reported different effects of the variation in upstream chloride concentration, (24,27,28,29). Since the upstream concentration was kept approximately constant, such effects were assumed negligible here. Rate of chloride migration

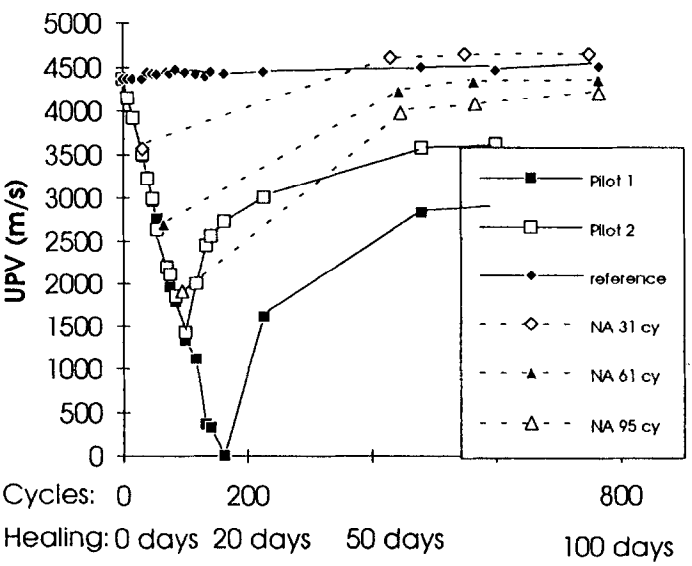

FIG. 2.
Freeze-thaw test and healing: Ultrasonic Pulse Velocity vs. time for the NA-concrete.

(dC/dt) and penetration time (t_0) were calculated by linear regression of the steady-state flow rate.

Results and Discussion

Air Void Characteristics (Table 1).. In NA the specific surface of the air voids (α) was very low, and the air void spacing factor ($\bar{L}$) very high, (α = 4.2 mm^{-1} and $\bar{L}$ = 1.10 mm). The air entrained mix A had α = 15.4 mm^{-1} and $\bar{L}$ = 0.23 mm, a significantly improved air void system for protection against rapid freeze/thaw exposure. The total air content varied somewhat between fresh and hardened concrete for mix NA, 3 and 5.7 % respectively, whereas in A it was 6.2 and 7.0 %. The high airvoid content of NA in hardened concrete might be due to compaction pores.

Ultrasonic Pulse Velocity (UPV). Figure 2 shows the evolution of the UPV for the NA-concrete during deterioration in freeze/thaw cycling, and at subsequent self-healing in water (8 cycles = 1 day). After 31, 61 and 95 cycles the NA-concrete had lost 18, 41 and 61 % UPV respectively. The A-concrete was well protected by the air entrainment, and had no loss of UPV after 95 and 316 cycles. The pilot specimens (NA-concrete) were run up to 160 cycles. Then, a complete loss of UPV was recorded. At this extreme stage of deterioration dense patterns of thin cracks could be seen on the surface of the specimens.

From figure 2 we also see that the recovery of UPV depends on how much the specimens were deteriorated, the more deteriorated the lower the recovery. For the least deteriorated specimens (31 cycles), more than 100 % recovery was measured. For specimen Pilot 1, which was freeze/thaw cycled to zero pulse velocity, only 55 % recovery was measured.

Compressive Strength. Table 3 shows compressive strength, as affected by freeze/thaw and subsequent healing in water.

For NA, freeze/thaw cycling reduced the strength to 68, 54 and 40 % of undamaged strength after 31, 61 and 95 cycles, respectively. Self healing increased the strength by 10 %, to 78 % of the initial value, for the concrete freeze/thaw exposed to 31 cycles. For the concretes exposed to 61 and 95 cycles no strength recovery was measured, even though the pulse velocity recovered significantly. The discrepancy between recovery of UPV and strength is in accordance with earlier experiences (1).

TABLE 4
Change in Volume, Mass (Vol-% of Concrete) and Density (kg/m^3) at Freeze/Thaw

		exposure				
		0 cy	31 cy	61 cy	95 cy	316 cy
NA	$\Delta V/V_0$ (vol-%)	0	0.7	1.7	2.9	-
	$\Delta m/m_0$ (vol-%)	0	1.0	1.9	2.9	
	Dens. (kg/m^3)	2.479	2.471	2.457	2.438	
A	$\Delta V/V_0$ (vol-%)	0	-	-	0	-0.1 1)
	$\Delta m/m_0$ (vol-%)	0			0	0
	Dens. (kg/m^3)	2.368			2.370	2.372

1) some surface scaling

Volume, Mass and Density. Table 4 shows changes in volume, mass and density of the cylinders during freeze/thaw exposure. The non-air entrained (NA) concrete had a rather linear increase in both volume and mass (water uptake). The values are significant, and indicate that the created crack volume is filled with water, since the volume increase equals volume of water absorbed. The volume increase due to internal cracking is in good accordance with previous measurements (1). Due to the increased volume and absorption of water, the density was reduced somewhat. For the undamaged air entrained (A) concrete, a small reduction of volume was measured due to a little surface scaling. The density of the A concrete (no frost damage) increased during freeze/thaw due to water absorption. During 300 cycles, 0.5 vol % absorption into paste or air voids was measured (without damage).

Crack Density. Table 5 gives the crack densities measured on the polished sections. The crack density (number of cracks traversing pr. unit line length) is clearly increased in the frost deteriorated concretes.

After freeze/thaw exposure, cracks were mostly seen in the interface between paste and aggregate, in accordance with earlier observations, (30). From 31 to 95 cycles the crack density increased steadily. Also the number of defects seen on the polished surfaces, such as ripped out aggregate particles, partly crushed zones and crack edges increased.

The concrete crack densities of 0.46 - 0.77 cracks pr. mm can be calculated on paste basis using a paste fraction of 0.28. This gives paste crack densities of 1.64 - 2.75 pr. mm, i.e. 0.61 - 0.36 mm distance between cracks. (No cracks were observed through aggregate particles). This is somewhat larger than the critical thickness T_{cr}, ($T_{cr} \cong 2 \times L_{cr}$) measured by Fagerlund (31) in hardened cement paste (HCP). He determined T_{cr} for virgin, saturated, well cured HCP of w/c = 0.4 experimentally to be 0.3 mm. The observation of cracks around a large number of aggregate particles already at the lowest degree of cracking, indicates that the aggregate (interface, elastic properties etc.) plays an important role in the cracking of concrete in rapid freeze/thaw tests.

Chloride Migration. Table 6 shows all test variables for chloride migration testing. The weight increase of the slices after a 2-day storage in water (vacuum or atmospheric pressure) prior to the chloride migration testing is also given. The vacuum treatment increases the water content in the cracked slices. The more cracking, the more water taken up at vacuum treatment. Prior to freeze/thaw exposure the air entrained concrete takes up more water during vacuum treatment than the non-air entrained. However, the quantity of water absorbed is very low compared to total air void content. Weight increase during three months of self healing was less than 0.05 vol. % for all three degrees of cracking. During subsequent vacuum saturation for two days of the healed slices, less water was absorbed than in the newly cracked slices. Therefore, the self healing appears to have reduced the accessibility of water to voids.

TABLE 5
Crack Densities Measured on Red Dye Impregnated Polished Sections

Specimen	Crack density (1/mm)		Description
	total	aggregate/paste	
NA 0 cy	0.09	0.08	
NA 31 cy	0.46	0.41	
NA 61 cy	0.61	0.52	Several aggregate particles ripped out
NA 95 cy	0.77	0.68	Several defects seen in surface

TABLE 6
Test Variables for Chloride Migration Testing

Concrete	Exposure	conditioning (2 days in water)	Water uptake (Vol-%)
freeze/thaw:	(cycles)		
NA-0-v	0	vacuum	0.0
NA-31-v	31	vacuum	0.5
NA-31-a	31	atmospheric	0.0
NA-61-v	61	vacuum	0.9
NA-61-a	61	atmospheric	0.1
NA-95-v	95	vacuum	1.5
healing:			
H-NA-31-v	90 days	vacuum	0.0
H-NA-61-v	in water	vacuum	0.1
H-NA-95-v		vacuum	0.7
freeze/thaw:	(cycles)		
A-0-v	0	vacuum	0.3
A-95-v	95	vacuum	0.1
A-316-v	316	vacuum	0.0

Table 7 gives data from chloride migration testing. The chloride migration rate (dC/dt, proportional to M) increases by 2.5, 4.3 and 7.9 times respectively after 31, 61 and 95 cycles compared to the virgin specimen. Time to penetrate through the specimen (t_0) is reduced from 64 hours (virgin) to 0 for the most cracked concrete. The specimens saturated at atmospheric pressure had somewhat lower rate of chloride migration than the vacuum saturated ones, showing that the water content/ degree of saturation has a significant influence on chloride migration in accordance with (24).

TABLE 7
Chloride Migration: dC/dt, t_o, r^2, (Regression), J (Flux) and M (Migration Coefficient)

Concrete	dC/dt mg Cl^-/(l·hr)	t_o hours	r^2	J x 10^{-10} mol/(cm^2·s)	M x 10^{-9} cm^2/s
Undamaged:					
NA-0-v	3.39 **(1)**	**64.3**	0.996	9.73	9.70
Damaged:					
NA-31-v 1)	8.56 **(2.5x)**	**24.2**	0.991	24.57	24.48
NA-31-a	6.41	25.2	0.980	18.40	18.33
NA-61-v	14.56 **(4.3x)**	**7.4**	0.997	41.79	41.64
NA-61-a	12.00	18.8	0.998	34.44	34.32
NA-95-v	26.66 **(7.9x)**	**0.1**	0.983	76.52	76.25
Healed:					
H-NA-31-v	6.03 **(1.8x)**	**44.2**	0.995	17.31	17.25
H-NA-61-v	10.36 **(3.1x)**	**27.2**	0.997	29.74	29.63
H-NA-95-v	17.23 **(5.1x)**	**3.0**	0.996	49.45	49.28
Air entrained:	(no damage)				
A-0-v	4.29	58.2	0.998	12.31	12.27
A-95-v	4.14	39.7	0.995	11.88	11.84
A-316-v	4.37	49.4	0.995	12.54	12.50

1) one slice only

Self healing leads to a significant reduction of (dC/dt), and increased t_0, compared to newly damaged (cracked) specimens. However, dC/dt is still higher and t_0 is lower than in the undamaged concrete. Note that also the concretes that had no self-healing in terms of compressive strength (61 and 95 cycles), had a reduction in dC/dt. The reduction in dC/dt due to healing, in percent of dC/dt in cracked concrete, is fairly equal for all three degrees of damage: 28 - 35 %. For the air-entrained concrete no significant effect of freeze/thaw on chloride migration can be deduced. It also appears that the chloride migration rate is a little higher in the air entrained than in the non-air entrained concrete.

Figures 3 and 4 show time vs. chloride concentration in the downstream cell. In each plot, both slices are shown. Figure 3 shows increasing slope (dC/dt) of the lines with increasing degree of internal cracking. Further, we see the effect of three months self healing: the slope is reduced for all concretes, though not down to the 0 cycles curve. Figure 4 shows that for the air entrained concrete there is no effect of 95 or 316 freeze/thaw cycles on rate of chloride migration.

The evolution of current during testing showed a small increase at the beginning of the test, and then stabilizing for the virgin and least cracked concretes. For the most cracked concrete a rather sharp increase was observed in the beginning, and then a gradual reduction again. For this (most cracked) concrete, production of chlorine gas was observed at the anode. This was not observed for the other less cracked concretes. One may speculate on the reason for this.

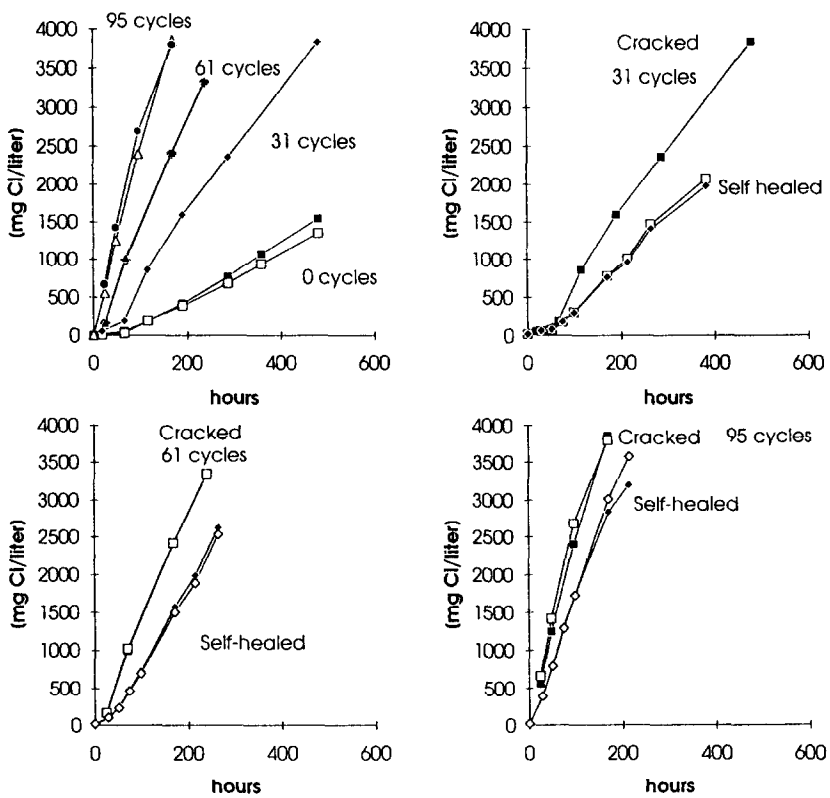

FIG. 3.
Effect of cracking and healing on chloride migration, Non air-entrained (NA) concrete.

Open cracks may have given more or less direct communication between the anode and the cathode. This apparently led to electrolysis, which may have changed significantly the conductivity of the solution. A thorough investigation of the electrochemical processes behind these observations lies beyond the scope of this paper, and will not be treated further here.

The migration coefficients obtained from these experiments have been compared with theoretical values given by a model. Gérard (32) has derived a set of equations relating mass transfer coefficient (M) in uncracked and cracked concrete assuming a cubical crack pattern, equation (3):

$$\frac{M_{cracked}}{M_{virgin}} = \frac{2}{d}\left(\frac{M_{H_2O}}{M_{virgin}}\right) + 1 \qquad (3)$$

In equation (3) $M_{cracked}$, M_{virgin} and M_{H2O} stand for migration coefficients in cracked and virgin concrete, and in water respectively, d = (crack distance /crack width) = crack spacing. M_{H2O} = 10^{-5} cm^2/s. The cracks are assumed water filled and parallel to the direction of flux, without tortuosity or surface roughness. The relation between volume increase and d is, Gérard (32):

$$\frac{\Delta V}{V_0} = \frac{d^3}{(d-1)^3} - 1 \qquad (4)$$

Table 8 shows a comparison between theoretical and measured increase in M due to cracking. The crack spacing d was calculated using the measured volume increase at freeze/thaw exposure. Mean crack widths were then calculated using measured crack densities. The calculated crack widths of 5 - 12 μm are in good accordance with the SEM observations in (2): 1 - 10 μm. The results of table 8 also point to that the measured volume increase and increased migration are more related to increased crack widths than to increased crack densities, since the (percentage) increase in crack width is larger than the increase in crack density.

By comparing measured and calculated increase in chloride migration in table 8, we see that the ratios theoretical/measured M are in the range 2.3 - 2.9. This must be considered as a good relationship, the calculated values being on the conservative side. The reasons for the deviation

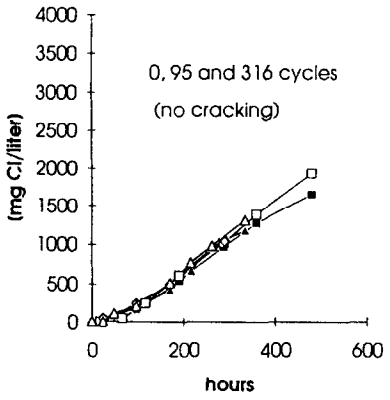

FIG. 4.
Effect of freeze/thaw cycling on chloride migration, Air entrained (A) concrete.

TABLE 8
Theoretical (Equation (3)) and Measured (Table 7) Increase of Migration

No. of cycles	$\Delta V/V_0$ (%) measured (table 4)	d 1) eq. (4)	crack density 1/mm (mm) measured (table 5)	crack width $\left(\frac{\text{density(mm)}}{d}\right)$	M_{crack}/M_{virgin} eq. (3)	measured	Ratio eq.(3)/ measured
0	0	0	0.09 (11.1)	-	1	1	1
31	0.7	440	0.46 (2.17)	5 µm	5.7	2.5	2.3
61	1.7	180	0.61 (1.64)	9 µm	12.5	4.3	2.9
95	2.9	105	0.77 (1.30)	12 µm	20.6	7.9	2.6

1) d (crack spacing) = distance between cracks/crack width

between theory and measured values are probably tortuosity effects/a more complex crack geometry than anticipated, and rugged crack surfaces.

Conclusions

Internal cracking reduced the compressive strength to 68 - 40 %, increased the chloride penetration rate 2.5 to 7.9 times and reduced the chloride penetration time through the 15 mm slices from 64 (undamaged) to 0 hours (most damaged). The cracks could be observed as increased volume of the specimen and dense crack patterns on polished sections. The cracks were seen to follow around a large portion of aggregate particles already at the lowest degree of damage. The increased chloride migration due to cracking correlated well with calculated increase using a square grid crack model with chloride ions migrating in water filled cracks.

Self healing of cracked concrete specimens for three months in water led to a significant reduction in rate of chloride migration: 28 - 35 % compared to migration in newly cracked specimens. Penetration time was significantly increased. The increase in compressive strength at self healing was very low: 0 - 10 % in spite of a 50 - 100 % recovery of UPV. 316 freeze/thaw cycles had no effect on chloride migration in the air entrained freeze/thaw durable concrete. The air entrainment increased the chloride migration slightly.

Acknowledgment

The research was carried out during a one year stay of the first author at Laval University/ CRIB. Thanks to: The Québec Ministry of Transportation (MTQ) for use of freeze/thaw chamber and press for compressive strength, Bruno Gérard for comments, Olivier Houdusse for preparation of the polished sections, the Norwegian Research Council for the scholarship, and Public Roads Laboratory (Veglaboratoriet), Norcem and Norwegian Contractors for financial support.

References

1. Jacobsen S., Sellevold E.J.: Cem. & con. res. Vol.26, 1, pp. 55-62 (1995)
2. Jacobsen S., Marchand J., Hornain H., Cem. & con. res. V.25, 8, pp. 1781-1790 (1995)

3. Jacobsen S., Sellevold E.J.: Conc. under severe conditions, Ch. & Hall, pp. 114-125 (1995)
4. Jacobsen S., Sellevold E.J., Matala S.: Paper acc. for publ. in Cem. & con. res. (1995)
5. Clear C.A.: Cement and Concrete Association Technical Report 559, England (1985)
6. Ripphausen B.: PhD thesis RWTH, Achen (1989) (In German)
7. Meichsner H.: Beton und stahlbetonbau 87, pp. 95 - 99 (1992) (In German)
8. Hearn N.: Ceramic Transactions, vol.16, pp.463 - 475, Ed.: S.Mindess (1990)
9. Arnold T. and Johnson D.: Proc. int. workshop on roller compacted concretes, CRIB-Université Laval, Québec, Canada pp.171-185 (1994)
10. Samaha H.R., Hover K.C.: ACI Materials Journal, V.89, No.4 pp.416-424 (1992)
11. Locoge P., Massat M., Ollivier J.P.: Cem. & con. res. Vol.22, nos.2/3, pp. 431-438 (1992)
12. Fidjestøl P., Nilsen N.: ACI SP-65 pp. 205-221 (1980)
13. Bakker R.F.M.: RILEM Report of the TC 60-CSC Chapman and Hall, pp. 22 - 54 (1988)
14. Sandberg P. and Tang L.: ACI SP-145 pp.557-571 (1994)
15. Dry C.: Smart Materials and Structures vol. 3 no. 2 pp.118-123, June (1994)
16. AASHTO T-161: Modified ASTM C666 test procedure, AASHTO, Washington D.C.
17. Hornain, H. and Regourd M.M.: 8th Int.congr.on the chemistry of cement, Rio de Janeiro, V-4, pp. 53-59 (1986) (In French)
18. AASHTO T 277-83, Standard method of test for resistance of concrete to chloride ion penetration, AASHTO, Washington D.C. (1983)
19. Nordtest method NT Build 355 Nordtest, Esbo, Finland (1989)
20. Luping T. Nilsson L-O.: ACI Materials Journal V.89 No.1 Jan.-Feb. pp. 49-53 (1992)
21. Streicher P.E., Alexander M.G.:3rd CANMET Dur. of Concr. Sup.papers pp. 517-530 (1994)
22. Andrade C.: Cem. & con. res. Vol.23 pp.724-742 (1993)
23. Andrade C., Sanjuán M.A., Recuero A., Rio O.: Cem. & con. res. Vol.24, no.6, 15 p. (1994)
24. Hauck C.: Dr.ing.thesis 1993:90, The Norwegian Institute of Technology (1993)
25. Nilsson L.O., Massat M. and Tang L.: ACI SP-145, pp. 469-486, (1994)
26. Gerard B., Marchand J.: Equilibres chimiques des materiaux cimentaires. Cinetique de transport. Internal report, Laval University December (1994) (In French)
27. Gérard, B., Marchand J. et Pigeon M.: Dégradation accélérée des bétons par champ électrique, Rapport EDF-Université Laval Québec, Canada Octobre (1994), 36.p (In French)
28. El-Belbol S.M.T.: PhD-thesis, Imperial College, London (1990)
29. Zhang T., Gjørv O.E.: Cem. & con. res., Vol.24, No.8, pp. 1534-1548 (1994)
30. Jacobsen S., Gran H.C., Sellevold E.J., Bakke J.A., Cem. & con. res.V.25, 8, pp. 1775-1780 (1995)
31. Fagerlund G.: Nordisk betong 2 pp.5 - 13 (1981) (In Swedish with English summary)
32. Gerard B.: Simulation de la diffusion equivalente d'un milieu fissuré. Internal report Laval University, December 13 p. (1994) (In French)